Journal of Southeast University (English Edition) Vol. 37, No. 3, pp. 258 - 263 Sept. 2021 ISSN 1003—7985

Buck converter stability techniques for secondary filters and adaptive voltage positioning

Yao Suyi Jiang Jianguo

(School of Electronic Information and Electrical Engineering, Shanghai Jiaotong University, Shanghai 200240, China)

Abstract: To reduce output voltage noise and improve dynamic response performance, this study designed a buck converter on the basis of secondary filters and adaptive voltage positioning (AVP). A hybrid control method was proposed for the compensation of the secondary filter. The introduction of a high-frequency feedback path, in addition to the traditional feedback path, effectively improved the influence of the secondary filter on the loop stability and direct current regulation performance. A small-signal model of the buck converter based on the proposed control method was derived, and the stability and selection of control parameters were analyzed. AVP is realized using an easy-to-implement and low-cost control method that was proposed to improve dynamic response performance by changing the low-frequency gain of the control loop and load regulation of the output voltage. The experimental results of the buck converter showed that the proposed method effectively reduced the output voltage noise by 50% and improved the dynamic response capability to meet the target requirements of mainstream electronic systems.

Key words: buck converter; secondary filter; adaptive voltage positioning (AVP); output voltage noise; small-signal model

DOI: 10.3969/j.issn.1003-7985.2021.03.004

With the gradual popularization of 5G and the growing demand for autonomous driving systems, buck converters with high power density and low noise have been widely used. At present, the radar systems in 5G communication systems and autonomous driving systems not only require large currents but also place high demands on the ripple and noise of the power supply. Noise can be reduced when a secondary filter is cascaded at the output of a buck converter. Small-signal models have been analyzed, and a guideline for the design of secondary filters has been proposed. However, a stability analysis of different secondary filters based on loop control has yet to be performed[1-2]. A fourth-order low-pass filter composed of equivalent inductance and external capacitance can be effectively used by designing printed circuit board (PCB) traces, but it can only filter out high-frequency noise [3]. On the basis of a delta-sigma modulator with a loop filter, noise can be successfully shaped, but the output ripple is still as high as 19 mV[4]. With the progress of semiconductor technology, the power supply voltage of core processors has decreased while current demand has increased. Hence, the accuracy requirements for the power supply have also increased. In the case of a large increase in load current transient response and slew rate, most processors currently require the total accuracy of the power supply to be within ±5% (static and dynamic). To improve dynamic system performance, studies have adopted AVP and have widely discussed the methods for its implementation. In addition to the output voltage feedback path, an additional AVP filter can be introduced to adjust the error amplifier reference in real-time, but it can easily result in output oscillation when the load jumps, and no specific analysis of loop stability has been conducted[5]. Adjusting load line resistance on the fly can effectively improve dynamic performance and direct current (DC) accuracy; however, doing so requires additional control circuits, such as transconductance amplifiers and voltage-controlled current sources, which also increase the complexity and cost of control[6-8]. A buck converter with digital control can eliminate current sampling through the current sensorless AVP mechanism, but it requires a high-precision analog-to-digital converter to obtain current information; hence, the complexity and cost of system development increase[9-10]. To reduce the effective value of noise integration in the frequency range of 10 to 1×10^5 Hz and optimize the noise spectrum density at a specific frequency while meeting the required output voltage dynamic performance and specific accuracy, the current study proposes a buck converter on the basis of a secondary filter and AVP control. Relative to the traditional buck converter, the proposed buck converter does not increase the complexity and cost of the control method, and it can effectively reduce the output voltage noise and enhance dynamic response performance. Meanwhile, a small-signal model of the control method is also presented, along with an analysis of loop stability and control circuit parameters. The feasibility of the scheme is verified by the modeling calculation and experimental results.

Received 2021-01-10, **Revised** 2021-07-10.

Biographies: Yao Suyi (1982—), male, Ph. D. candidate; Jiang Jianguo (corresponding author), male, doctor, professor, jjg6722@163.com.

Citation: Yao Suyi, Jiang Jianguo. Buck converter stability techniques for secondary filters and adaptive voltage positioning [J]. Journal of Southeast University (English Edition), 2021, 37(3): 258 - 263. DOI: 10.3969/j.issn.1003-7985.2021.03.004.

1 Buck Converter with Secondary Filter

1.1 System architecture

To reduce the output noise of a buck converter, a second-stage filter can be cascaded after the output LC filter, which can substantially reduce the noise generated by the switching frequency and higher harmonics. However, adding a second-stage filter affects loop stability and DC regulation. As shown in Fig. 1, the remote feedback method uses the output of the second-stage filter as a feedback node, which has good DC regulation performance. However, the loop bandwidth is too small and thus directly affects the stability and dynamic response performance. Another approach is the local feedback method, which uses the input of the second-stage filter as the feedback node. Although this method can improve the loop bandwidth and dynamic response performance, the impedance of the PCB trace and the DCR of the second-stage inductor causes a voltage drop with the load, thereby affecting DC regulation.

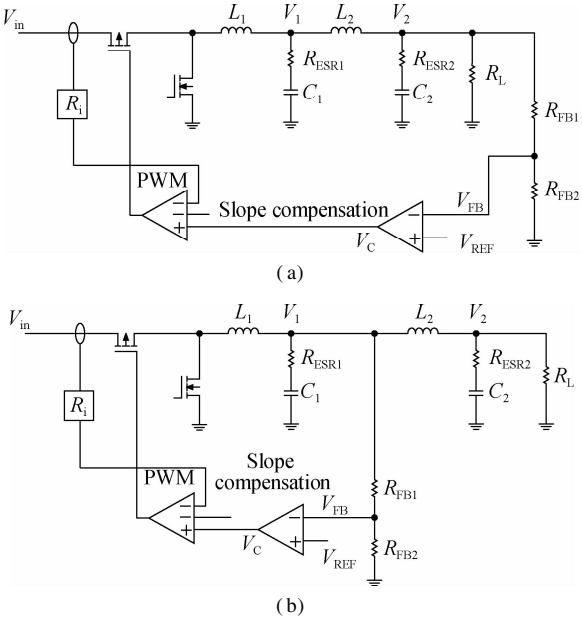

Fig. 1 Buck converter with secondary filter. (a) Remote feedback; (b) Local feedback

To improve the DC regulation and loop stability, this study proposes a hybrid feedback control method (see Fig. 2). The hybrid feedback control method not only guarantees DC regulation with the remote feedback method but also improves loop stability and dynamic response performance by adding high-frequency feedback paths C_F and R_F.

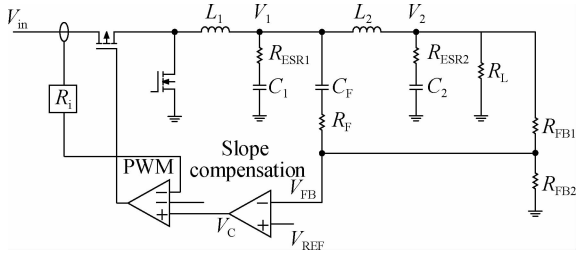

Fig. 2 Buck with secondary filter and hybrid feedback

1.2 Small-signal analysis

In this study, a small-signal model of the secondary filter of the buck converter is derived on the basis of the peak current mode buck converter to analyze the influence of the hybrid feedback method on stability and to design a high-frequency feedback path. The control loop diagram is shown in Fig. 3. G_{F1} is the high-frequency feedback path transfer function from local output V_1 to V_{FB}. G_{F2} is the low-frequency feedback path transfer function from remote output V_2 to V_{FB}. G_{v1d} and G_{v2d} are the transfer functions of the output voltages V_1 and V_2 to the duty cycle, respectively.

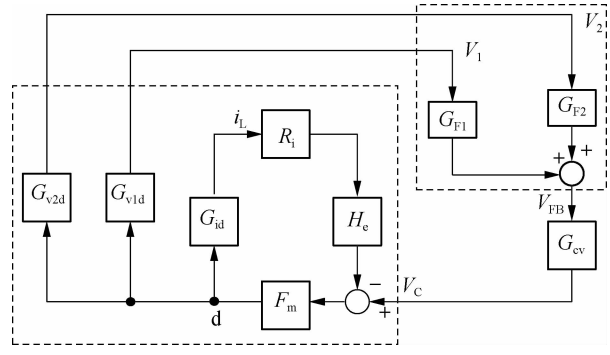

Fig. 3 Small-signal model of peak current mode buck converter with secondary filter and hybrid feedback

The output impedance Z_1 of V_1 is

$$Z_1 = \frac{1 + R_1 C_1 s}{C_1 s} \tag{1}$$

The output impedance Z_2 of V_2 is

$$Z_2 = \frac{R_L(1 + R_2 C_2 s)}{1 + R_L C_2 s + R_2 C_2 s} \frac{1 + R_1 C_1 s}{C_1 s} \tag{2}$$

The transfer function of local output V_1 to the inductor current is

$$G_{v1i} = \frac{Z_1(L_2 s + Z_2)}{Z_1 + L_2 s + Z_2} \frac{1 + R_1 C_1 s}{C_1 s} \tag{3}$$

The transfer function of remote output V_2 to the inductor current is

$$G_{v2i} = \frac{G_{v1i} Z_2}{L_2 s + Z_2} \frac{1 + R_1 C_1 s}{C_1 s} \tag{4}$$

The transfer function of the inductor current to the duty cycle is

$$G_{id} = \frac{V_{in}}{L_1 s + G_{v1i}} \frac{1 + R_1 C_1 s}{C_1 s} \tag{5}$$

The transfer functions of the output voltages V_1 and V_2 to the duty cycle are given, respectively, as

$$G_{v1d} = G_{id} G_{v1i} \frac{1 + R_1 C_1 s}{C_1 s} \tag{6}$$

$$G_{v2d} = G_{id} G_{v2i} \frac{1 + R_1 C_1 s}{C_1 s} \tag{7}$$

The transfer function of the current inner loop is

$$T_i = F_m G_{id} R_i H_e \frac{1 + R_1 C_1 s}{C_1 s} \tag{8}$$

Thus, the transfer functions of the output voltages V_1 and V_2 to the control node V_C can be respectively derived as

$$G_{v1c} = \frac{F_m G_{v1d}}{1 + T_i} \frac{1 + R_1 C_1 s}{C_1 s} \tag{9}$$

$$G_{v2c} = \frac{F_m G_{v2d}}{1 + T_i} \frac{1 + R_1 C_1 s}{C_1 s} \tag{10}$$

where G_{v1c} and G_{v2c} are the control-to-output (V_1 and V_2, respectively) transfer functions.

Therefore, the loop gain is

$$T = (G_{v1c} G_{F1} + G_{v2c} G_{F2}) G_{cv} \frac{1 + R_1 C_1 s}{C_1 s} \tag{11}$$

$$T = G_{v2c}(KG_{F1} + G_{F2}) G_{cv} = G_{v2c} G_{FB} G_{cv} \frac{1 + R_1 C_1 s}{C_1 s} \tag{12}$$

Here, G_{CV} is the error amplifier compensator transfer function, and K is the ratio of G_{V1C} and G_{V2C}.

$$G_{FB} = G_{F2} + G_{F1} K \tag{13}$$

$$K = \frac{G_{v1c}}{G_{v2c}} = \frac{G_{v1d}}{G_{v2d}} \tag{14}$$

$$G_{F1} = \frac{\dfrac{1}{Z_F}}{\dfrac{1}{R_{FB1}} + \dfrac{1}{R_{FB2}} + \dfrac{1}{Z_F}} \tag{15}$$

$$G_{F2} = \frac{\dfrac{1}{R_{FB1}}}{\dfrac{1}{R_{FB1}} + \dfrac{1}{R_{FB2}} + \dfrac{1}{Z_F}} \tag{16}$$

$$Z_F = R_F + \frac{1}{sC_F} \tag{17}$$

The feedback transfer function G_{FB} has one conjugate zero pair f_Z, and the control transfer G_{v2c} has one conjugate pole pair f_P, as shown in the following equations:

$$f_z = \frac{1}{2\pi \sqrt{\dfrac{L_2 C_2 R_{FB1}}{R_{FB1} + R_F}}} \tag{18}$$

$$f_p = \frac{1}{2\pi \sqrt{\dfrac{L_2 C_1 C_2}{C_1 + C_2}}} \tag{19}$$

The conjugate zero pair is made to cancel the conjugate pol part to reduce the impact on the loop control. R_F can be expressed as

$$R_F = R_{FB1} \frac{C_2}{C_1} \tag{20}$$

Fig. 4 shows the gain and phase of G_{FB}. If the value of C_F is too small, then the zero pair in G_{FB} moves to the right half plane, thus causing a 180° phase delay and instability. To keep the zero-point pair on the left half plane, the following requirement needs to be met:

$$C_F > \frac{\dfrac{C_2 L_2}{R_{FB1} + R_F}}{\dfrac{L_2}{R_L} + C_2 R_{ESR2}\left(1 + \dfrac{R_F}{R_{FB1}}\right)} \tag{21}$$

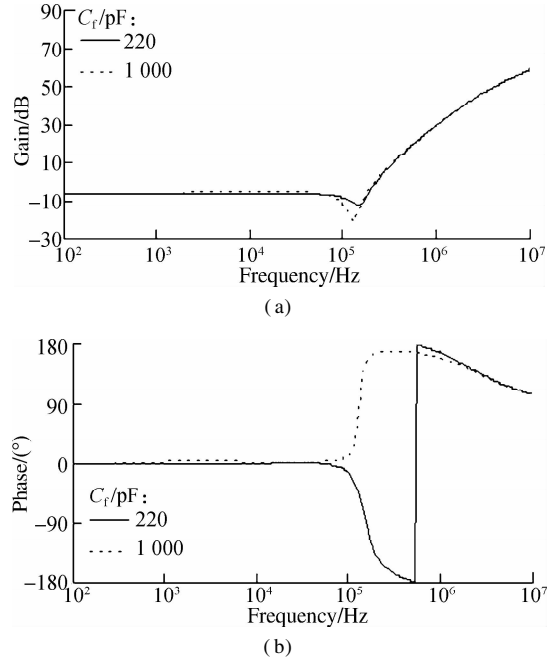

Fig. 4 Hybrid feedback transfer function G_{FB} of the secondary buck converter. (a) Gain; (b) Phase

Fig. 5 shows the gain and phase of the loop gain T. If the value of C_F is too small, then the zero pair in G_{FB} moves to the right half plane, thereby causing a 180° phase delay and instability.

2 Buck Converter with AVP Control

To reduce the fluctuation of the output voltage when the load jumps, this study proposes a low-cost and easy-to-implement AVP control method (see Fig. 6). By adding a load line resistor between the output voltage feedback node V_{FB} and the output of the error amplifier, the low-frequency gain of the loop is reduced to increase

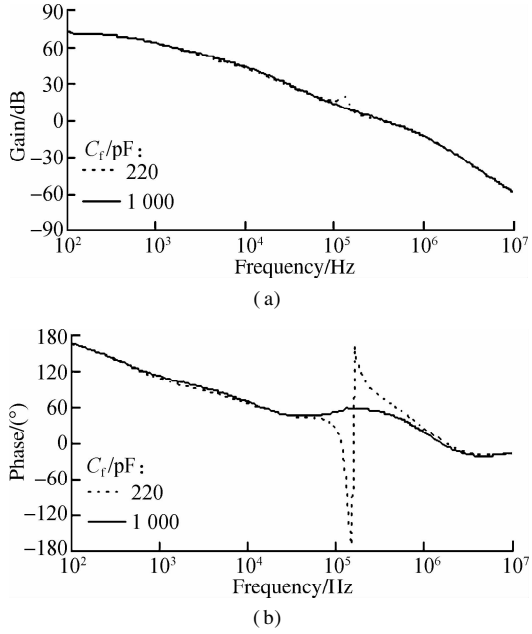

Fig. 5 Loop gain transfer function of the secondary buck converter. (a) Gain; (b) Phase

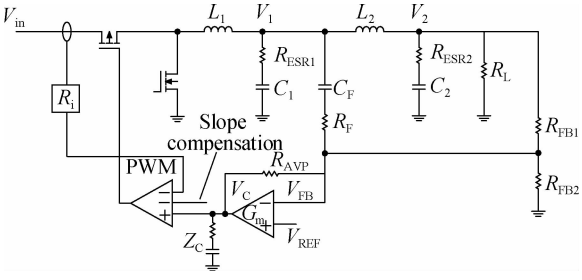

Fig. 6 Buck converter based on AVP control

the load regulation of the output voltage and thereby optimize the dynamic response of the output voltage.

The AVP control method is analyzed using a small-signal model that obtains the loop transfer function and its influence on loop stability. AVP control differs from the conventional control loop in terms of the error amplifier. In this work, the equivalent circuit is altered to facilitate the analysis(see Fig. 7) .

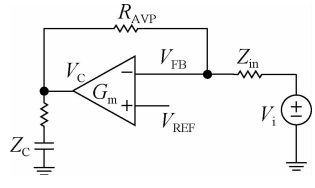

Fig. 7 Equivalent control diagram of error amplifier with AVP

The following formulas can be obtained by analyzing the virtual short and virtual break of the amplifier.

$$V_C = \left(-G_m V_{FB} - \frac{V_C - V_{FB}}{R_{AVP}} \right) Z_C \tag{22}$$

$$\frac{V_i - V_{FB}}{Z_{in}} + \frac{V_c - V_{FB}}{R_{AVP}} = 0 \tag{23}$$

Here, Z_{in} is the equivalent input impedance of the amplifier.

$$Z_{in} = \frac{R_{FB1} R_{FB2}}{R_{FB1} + R_{FB2}} \tag{24}$$

The input to the control transfer function of the error amplifier can be derived as

$$\frac{V_C}{V_i} = \frac{Z_C - G_m R_{AVP} Z_C}{R_{AVP} + Z_C + Z_{in} + G_m Z_{in} Z_C} \tag{25}$$

$$V_i = \frac{R_{FB2}}{R_{RF1} + R_{FB2}} V_O \tag{26}$$

Eq. (26) is substituted into Eq. (25), and the output to the control transfer function is

$$\frac{V_C}{V_O} = \frac{R_{FB2}(Z_C - G_m Z_C R_{AVP})}{(R_{FB1} + R_{FB2})(R_{AVP} + Z_C + Z_{in} + G_m Z_C Z_{in})} \tag{27}$$

The loop gain of the AVP buck converter is

$$T = G_{VC} \frac{V_C}{V_O} \tag{28}$$

where G_{VC} is the control for the output transfer function given as

$$G_{VC} = \frac{F_m G_{vd}}{1 + T_i} \tag{29}$$

From the perspective of amplitude frequency characteristics (see Fig. 8) , the control loop transfer function only reduces the low-frequency gain without affecting the loop bandwidth. Similarly, the phase frequency characteristics only change the low-frequency phase without affecting the phase margin of the loop. It facilitates the design of the compensator without increasing the complexity of the control loop and the system cost.

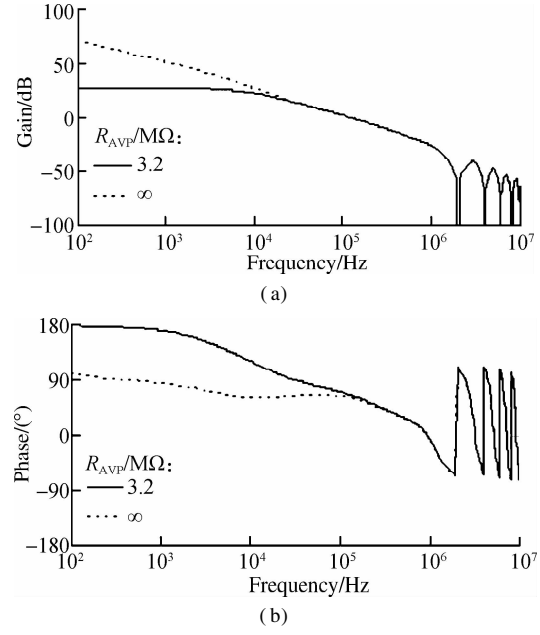

Fig. 8 Loop gain T of the buck converter with AVP. (a) Gain; (b) Phase

The selection of the value of R_{AVP} is discussed herein. Assuming that the system requires ΔV_{O_MAX} as the output voltage accuracy specification, the output deviation ΔV_{O_TR} is caused by the dynamic load without R_{AVP}. The load regulation changes ΔV_{O_LR} caused by R_{AVP} can be obtained by

$$\Delta V_{O\_MAX} = \Delta V_{O\_TR} - \Delta V_{O\_LR} \tag{30}$$

The closed-loop output impedance is

$$R_{LR} = \frac{R_L}{1 + |T|} \tag{31}$$

The low frequency gain of the loop gain is

$$|T| = \frac{R_{AVP} G_m - 1}{1 + Z_{in} G_m} \tag{32}$$

The load regulation can be calculated by

$$\Delta V_{O\_LR} = I_O R_{LR} = \frac{V_O (1 + Z_{in} G_m)}{G_m (R_{AVP} + Z_{in})} \tag{33}$$

Thus, the value of R_{AVP} can be derived as

$$R_{AVP} = \frac{V_O (1 + Z_{in} G_m)}{G_m \Delta V_{O\_LR}} - Z_{in} \tag{34}$$

3 Experimental Results

The prototype is based on a 10 A, 8 MHz buck converter with a secondary filter and AVP control for experimental analysis. The prototype specifications are listed in Tab. 1.

Tab. 1 Prototype specifications

Parameter	Value
V_{in}/V	3.3
V_O/V	1.0
Inductor/nH	100
Output capacitor/μF	47
Secondary filter/nH	220
Hybrid feedforward/kΩ	15
Error amplifier gain/μS	800
Compensation resistor/kΩ	30
Compensation capacitor/pF	20
AVP resistor/MΩ	3.2

The results of the noise spectral density are shown in Fig. 9(a), and the integrated noise of the specific frequency range can be obtained accordingly. The output noise can be suppressed, especially when the frequency exceeds 1 MHz, that is sensitive for the downstream devices. Fig. 9(b) shows a 30 mV peak-to-peak output ripple without the secondary filter and a small 1.7 mV peak-to-peak output ripple with the secondary filter.

The comparison of the dynamic response results demonstrates that AVP control effectively improves the output

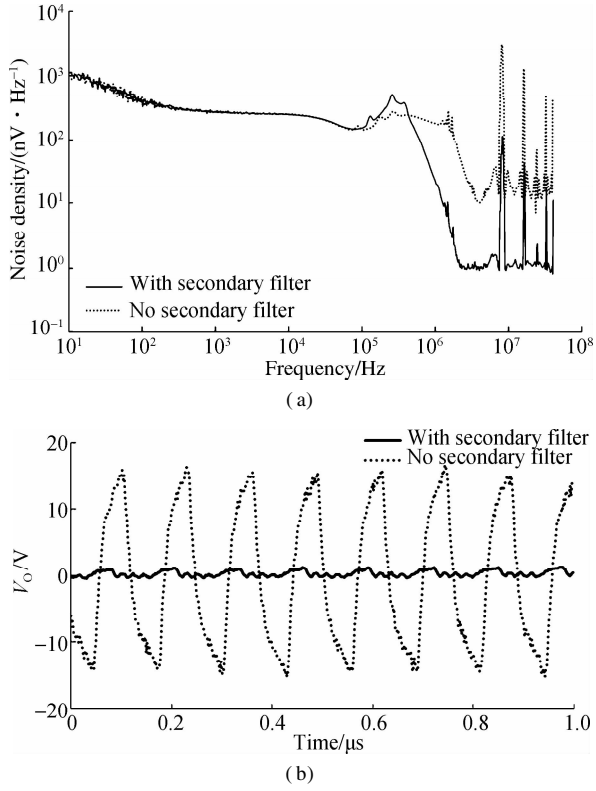

Fig. 9 Comparison of output voltage with and without the secondary filter. (a) Output noise density; (b) Output ripple

voltage dynamic response (see Fig. 10). The experimental results show that load regulation increases by 3%, but the output deviation caused by the load step improves by 2%. Therefore, the output voltage accuracy (static and dynamic) meets the 5% accuracy requirement of downstream devices. In other words, the buck converter requires minimal output capacitance and therefore reduces system cost.

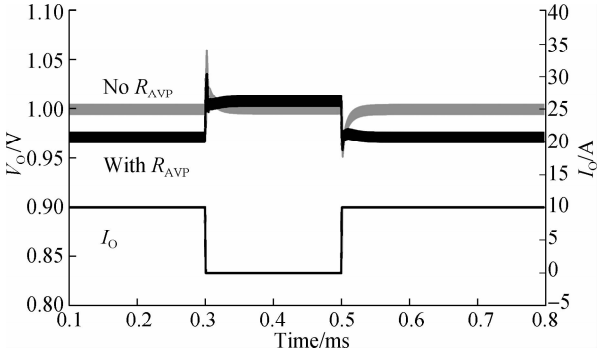

Fig. 10 Comparison of load transient with and without R_{AVP}

4 Conclusions

1) Current electronic systems have increased requirements for the accuracy and noise of the output voltage of the power supply. Hence, this study proposes a buck converter architecture on the basis of a secondary filter and AVP control.

2) Small-signal models are proposed for the two con-

trol methods. The hybrid feedback control and AVP control parameter values are derived accordingly for loop stability analysis.

3) The calculation and experimental results of the buck converter verify the effectiveness of the proposed control method. Moreover, the experimental results show that the noise of the output voltage can be reduced obviously, especially when the frequency is greater than 1 MHz. The dynamic response of the output voltage can be improved by 2%, which meets the required 5% accuracy for the power supply in most mainstream electronic systems.

References

[1] Ridley R B. Secondary LC filter analysis and design techniques for current-mode-controlled converters [J]. *IEEE Transactions on Power Electronics*, 1988, **3**(4): 499 – 507. DOI: 10.1109/63.17972.

[2] Sanal E, Dost P, Sourkounis C. LCL-Filter design for a battery charger based on buck converter (DCDC converter) [C]// *IEEE International Conference on Renewable Energy Research and Applications* (*ICRERA*). Birmingham, UK, 2016: 101 – 110. DOI: 10.1109/ICRERA.2016.7884408.

[3] Tang N, Nguyen B, Molavi R, et al. Fully integrated buck converter with fourth-order low-pass filter [J]. *IEEE Transactions on Power Electronics*, 2017, **32**(5): 3700 – 3707. DOI: 10.1109/TPEL.2016.2593049.

[4] Cho Y K, Kim M D, Kim C Y. A low switching noise and high-efficiency buck converter using a continuous-time reconfigurable delta-sigma modulator [J]. *IEEE Transactions on Power Electronics*, 2018, **33**(12): 10501 – 10511. DOI: 10.1109/TPEL.2018.2806360.

[5] Jiang Y J, Fayed A. A buck converter with optimized dynamic response using lag-lead active voltage positioning [C]// *IEEE 60th International Midwest Symposium on Circuits and Systems* (*MWSCAS*). Boston, MA, USA, 2017: 11 – 18. DOI: 10.1109/MWSCAS.2017.8052954.

[6] Chen C J, Lu S H, Hsiao S F, et al. A current-mode buck converter with reconfigurable on-chip compensation and adaptive voltage positioning [J]. *IEEE Transactions on Power Electronics*, 2019, **34**(1): 485 – 494. DOI: 10.1109/TPEL.2018.2827949.

[7] Tsai C H, Chen B M, Li H L. Switching frequency stabilization techniques for adaptive on-time controlled buck converter with adaptive voltage positioning mechanism [J]. *IEEE Transactions on Power Electronics*, 2016, **31**(1): 443 – 451. DOI: 10.1109/TPEL.2015.2405339.

[8] Lee M, Chen D, Huang K, et al. Modeling and design for a novel adaptive voltage positioning (AVP) scheme for multiphase VRMs [J]. *IEEE Transactions on Power Electronics*, 2008, **23**(4): 1733 – 1742. DOI: 10.1109/TPEL.2008.924822.

[9] Hu K Y, Chen B M, Tsai C. A digitally controlled buck converter with current sensor-less adaptive voltage positioning (AVP) mechanism [C]// *International Symposium on VLSI Design, Automation and Test*. Hsinchu, China, 2017: 332 – 341. DOI: 10.1109/VLSI-DAT.2017.7939664.

[10] Hu K Y, Tsai C H, Tsai C W. Digital V2 constant on-time control buck converter with adaptive voltage positioning and automatic calibration mechanism [J]. *IEEE Transactions on Power Electronics*, 2021, **36**(6): 7178 – 7188. DOI: 10.1109/TPEL.2020.3039061.

基于二次滤波器和自适应电压调节的降压变换器稳定性技术

姚苏毅　姜建国

(上海交通大学电子信息与电气工程学院, 上海 200240)

摘要: 为降低输出电压噪声,改善动态响应性能,设计了一种基于二次滤波器和自适应输出电压调节(AVP)的降压变换器. 针对二次滤波器的补偿,提出了一种混合控制方式. 在传统的反馈环节外,增加一个高频通路环节,有效改善了二次滤波器对环路稳定性和直流调节性能方面的影响. 推导出基于该控制方法的降压变换器的小信号模型,并对其稳定性和控制参数的选取进行了分析. 为了实现自适应输出电压调节,提出了一种易于实现且低成本的控制方法,通过改变控制环路低频增益和输出电压负载调整率来改善动态响应性能. 降压变换器原型试验结果表明,所提方法可有效降低50%的输出电压噪声,同时改善了动态响应能力,达到目前主流电子系统的指标需求.

关键词: 降压变换器;二次滤波器;自适应电压调节;输出电压噪声;小信号模型

中图分类号: TM46